

## **Synthesis and Characterization of Nanostructured CuO/CeO<sub>2</sub> Catalysts via Ultrasound Assisted Techniques used for Selective Oxidation of CO**

*A. Karimi, E. Fatehifar\*, R. Alizadeh*

*Environmental Engineering Research Center (EERC), Faculty of Chemical Engineering, Sahand University of Technology, Sahand New Town, Tabriz, Iran*

### **Abstract**

*In this study, CuO/CeO<sub>2</sub> Nano-catalyst was successfully prepared by impregnation-ultrasound assisted methods and used for selective oxidation. This catalyst has been characterized by means of XRD, BET, FTIR and SEM. The results show that CuO/CeO<sub>2</sub> is nanosized ( $r_{SEM} < 100$  nm) and BET surface area of tested materials was in the range of 45–76 m<sup>2</sup>/g. CuO is the active phase for selective CO oxidation, even operating at a gas hourly space velocity as high as 30000 h<sup>-1</sup>. The catalysts CuO/CeO<sub>2</sub> exhibit the CO conversion 100% in the wide temperature range of 100–120 °C, and with the CO oxidation selectivity greater than 86% at 100 °C.*

**Keywords:** *Nanocatalyst, Selective Oxidation, Copper Oxide Ceria, Ultrasound Energy*

### **1. Introduction**

Hydrogen gas can be produced from natural gas, steam reforming of methanol for various applications such as ammonia production, hydrocracking, hydrodesulfurization, hydrodealkylation and polymer electrolyte membrane fuel cell (PEMFC). The reformate gases contain about 50% H<sub>2</sub>, 20% CO<sub>2</sub>, 0.5–1% CO, 10% H<sub>2</sub>O and N<sub>2</sub> [1]. As the catalyst is used in the refinery and petrochemical plants will be contaminated by CO even at low levels of 10–100 ppm, and

fuel cells are highly sensitive to even trace amounts (<50 ppm) of CO, gas separation and purification stages must be followed for reforming [2]. Therefore, as much carbon monoxide as possible must be removed. Catalytic selective CO oxidation and catalytic methanation are the only choices to decrease CO concentration to satisfactory levels. Among the mentioned techniques, catalytic selective oxidation of CO seems to be the most straightforward and cost impressive procedure to achieve suitable CO

---

\* Corresponding author: fatehifar@sut.ac.ir

concentrations [3]. The catalyst used in the preferential CO oxidation (PROX) reaction should display superior catalytic activity and a high selectivity for the CO oxidation, and also an effective PROX reaction to reduce consumption of the H<sub>2</sub>. Several catalysts have been proposed in the literature for the selective oxidation of CO in excess H<sub>2</sub>. The main reactions occurring in PROX are:

Desired reaction:  $\text{CO} + 0.5\text{O}_2 \rightarrow \text{CO}_2 + 67.6$   
(kcal/mol)

Undesired reaction:  $\text{H}_2 + 0.5\text{O}_2 \rightarrow \text{H}_2\text{O} + 58.6$   
(kcal/mol)

Both reactions are exothermic, irreversible and competitive. The current catalysts for CO PROX are based on late transition metals such as platinum group metals (Pt, Pd, Ru and Rh) catalysts [4-8], gold-based catalysts [9-11], and recently transition metal-based catalysts (Cu, Co and Mn) [12-14] have also been used. The CuO/CeO<sub>2</sub> represents one of the most interesting catalysts, which has resulted in more active, selective and convenient thermally stable catalysts than Pt or Au based [15-17]. The absence of precious metals in the composition of these catalysts is a remarkable economic advantage. In this research, CuO/CeO<sub>2</sub> catalysts were prepared by the impregnation-ultrasound method and their catalytic performance was tested for PROX of CO in H<sub>2</sub>-rich gas streams. This synthesis method has been chosen for the following reasons. Due to turbulent flow and shock waves, metal particles can move toward each other at high-speed and may also melt in collision point [18]. The suspension solution occurs because of very quick Inter-particle

collisions, as a result, the mass of the particle is formed. Collisions can cause a crushing blow between particles, and so, increased specific surface, and finally to achieve high reactivity and good conversion. The impregnation-ultrasound method in comparison with other methods such as sol-gel [19], co-precipitation and impregnation [16] has high specific surface, also finer particles that confirm SEM pictures.

## **2. Experimental**

### **2-1. Catalyst preparation**

The impregnation-ultrasound method was used for preparation of the CuO/CeO<sub>2</sub> Nano-catalysts. Cu (NO<sub>3</sub>)<sub>2</sub>·3H<sub>2</sub>O, Ce (NO<sub>3</sub>)<sub>3</sub>·6H<sub>2</sub>O (both from Merck) were used as metal precursors. All the metal salts in the amounts required for a catalyst were dissolved in 100 mL de-ionized water and mixed for CuO/CeO<sub>2</sub> catalysts with proper amounts, for synthesis of catalysts Bandelin model 3200 ultrasound apparatus was used. The power of 70 w is considered for a homogeneous sample. The solution took over 40 minutes under the influence of ultrasound waves. As the temperature of metal salt solution is increased during the process, ice-water bath was used till temperature of the solution was reduced and the temperature was kept constant at 35°C, for evaluation of catalysts, CuO/CeO<sub>2</sub> catalysts have been synthesized to compare previous work [20]. The catalysts were subsequently dried at 110°C for 48 h and finally calcined for 5 h at 500°C under air flow at a given heating rate (h.r.=10°C/min). The algorithm of synthesis was indicated in Fig. 1.

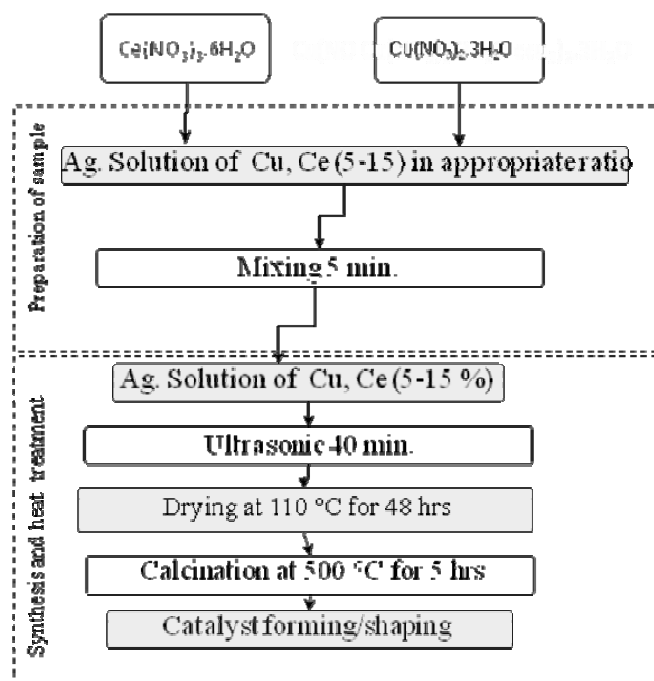


Figure 1. The schematic diagram of catalyst synthesis.

## 2-2. Catalyst characterization

The specific surface areas of the catalysts ( $S_{BET}$ ) were measured by means of nitrogen physisorption at  $-196^{\circ}\text{C}$  using a Quantachrome ChemBET3000 instrument. The crystalline structure of the catalysts was analyzed by means of X-ray powder carried out by D5000 Siemens device 30 kV and 20 mA with scan rate  $0.04\text{ s}^{-1}$ . The average crystallite sizes were calculated from the peak width using Scherrer's equation [20].

$$D = 0.9\lambda / (\beta\cos\theta) \quad (1)$$

Fourier Transform Infrared (FTIR) was used to identify organic functional groups. FTIR spectra of catalysts were prepared in a Unicam Mattson 1000 spectrometer, and were recorded with potassium bromide pressed discs. Catalyst morphology was examined using JEM100CX scanning electron microscope (SEM) and all of the

samples were first sputtered with Au for several minutes. The electron gun was operating at a voltage of 15 kV for the collection of all images.

## 2-3. Catalyst activity test

The catalytic oxidation of CO was carried out in a fixed-bed reactor system at atmospheric pressure (with the difference being that reactor is placed out of furnace, in most of the pilots fixed-bed reactor is placed in the furnace). All inlet gases were heated in furnace, and then passed through to reactor. The reactor was a 4 mm I.D. (6-mm O.D.). Prior to all catalytic tests, the samples were heated in a flowing 20 vol.%  $\text{O}_2/\text{N}_2$  mixture at  $300^{\circ}\text{C}$  for 40 min as a standard pretreatment, followed by cooling down to the reaction temperature in pure  $\text{N}_2$ . The catalyst weight was 200-300 mg and the total flow rate of the reaction mixture consisted of 1 vol.% CO, 1 vol.%  $\text{O}_2$  and 50 vol.%  $\text{H}_2$  in

N<sub>2</sub> balance was adjusted to 200-400 mL.min<sup>-1</sup>. The gas lines were heated, in order to avoid water condensation before the reactor inlet. The reactor effluent was passed through an ice-cooled water condenser to remove water vapor before inlet GC for analysis. Reactant and product components were analyzed online by a gas chromatograph (Agilent Technologies 7890A Network GC system) equipped with a thermal conductivity detector (TCD) that was used to analyze the outlet composition. HP-Plot Q column (Agilent) was used, with helium as carrier. The CO conversion was based on the carbon monoxide consumption in the reaction as follows:

$$Activity (\%) = \frac{[CO_2]_{out}}{[CO_2]_{out} + [CO]_{out}} \times 100$$

The selectivity is defined as the oxygen consumed by CO oxidation, namely:

$$Selectivity (\%) = \frac{0.5[CO_{in} - CO_{out}]}{[O_2]_{in} - [O_2]_{out}} \times 100$$

### 3. Results and Discussion

Catalysts were characterized by using different techniques. N<sub>2</sub> physisorption measurements (BET) were made in order to obtain the surface areas, XRD technique was used in order to obtain the phases present in the catalysts. Fourier Transform Infrared (FTIR) spectroscopic is one of the most useful techniques to identify and measure organic functional groups and inorganic ions. SEM results showed the surface morphology of the catalysts, and the activity measurements of the catalysts to CO oxidation reactions illustrate the relationship between the characteristic properties of the catalysts with activity. BET surface area and particle sizes of catalysts are shown in Table 1. BET surface areas of the 5 and 15% CuO/CeO<sub>2</sub>, 76 and 45 respectively, were observed with increase of loading. Cu decreased specific surface areas of the catalysts. The reason can be active phase on surface of the support that causes surface area to be reduced. A simple geometrical approximation of the BET analysis used to obtain particle size showed that synthetic catalysts are nanometer in size [21].

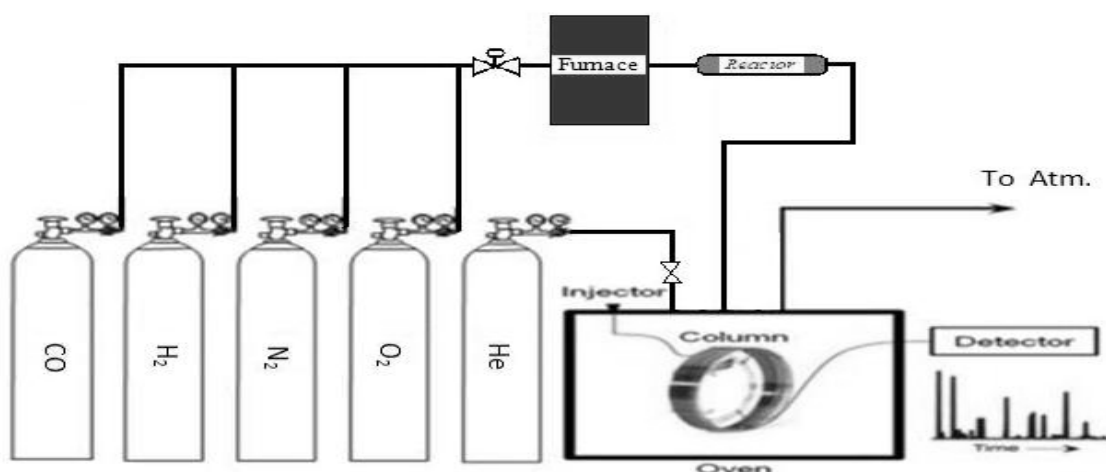


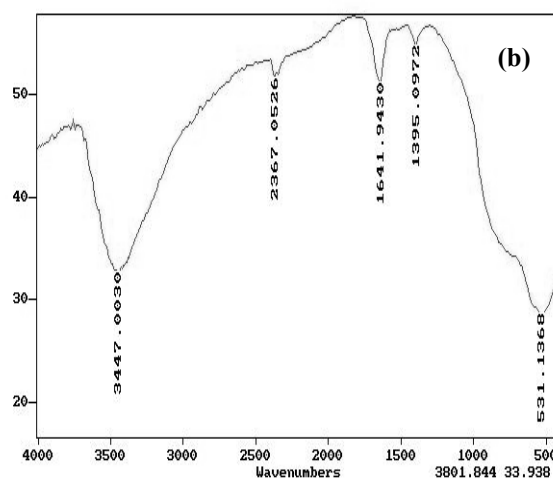
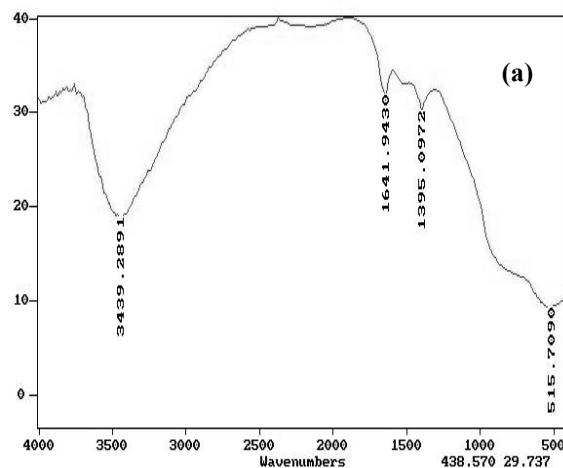
**Figure 2.** Schematic diagram of the experimental setup.

**Table 1.** Surface area and particle sizes of prepared catalysts.

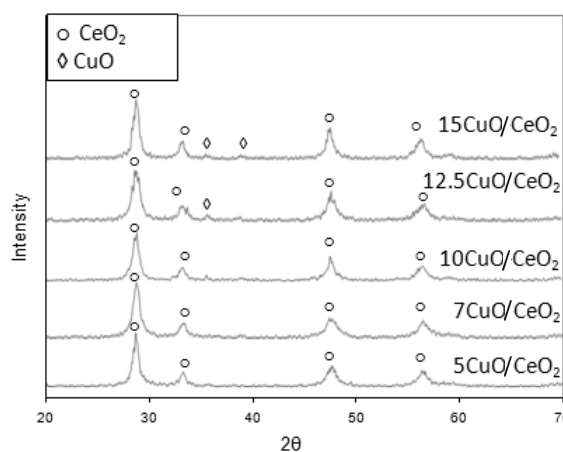
Catalyst	Surface area (m <sup>2</sup> /gr)	Particle size (nm)
%5 CuO/CeO <sub>2</sub>	76	45
%7 CuO/CeO <sub>2</sub>	63	50
%10 CuO/CeO <sub>2</sub>	57	53
%12.5 CuO/CeO <sub>2</sub>	53	55
%15 CuO/CeO <sub>2</sub>	45	60

The functional groups of synthesis catalysts are indicated in Fig. 3. The peaks area 400-500 cm<sup>-1</sup> is of oxidized metals such as Mg, Ni, Co, Cu. So the wave number of the peak can be attributed to the Cu-O bond vibrations. The wave number 1650 cm<sup>-1</sup> is bending vibration O-H of adsorbed water bond and absorption bands in 3200-3600cm<sup>-1</sup> are hydrogen bonds which indicate the amount of moisture is absorbed in the air by the sample.

The X-ray diffraction results of the CuO/CeO<sub>2</sub> catalysts after calcination are shown in Fig. 4. All the catalysts exhibited the characteristic CeO<sub>2</sub> cubic fluorite structure in the 2θ region of 25-58° characteristic. The crystal size of nano-catalysts synthesized by the impregnation-ultrasound method is shown in Table 2. The size of the crystal produced is obtained from Scherrer's equation. The XRD patterns of the CuO/CeO<sub>2</sub> catalysts showed no CuO reflections in less than 12.5% loading of Cu, indicating that the copper oxide phase exists in a highly divided or amorphous state in these specimens. The absence of CuO peaks may be attributed to, fine dispersion of CuO on the surface of ceria [22–24].



**Figure 3.** FTIR photographs of fresh CuO/CeO<sub>2</sub> catalysts (a) %10 CuO, (b) %7 CuO.



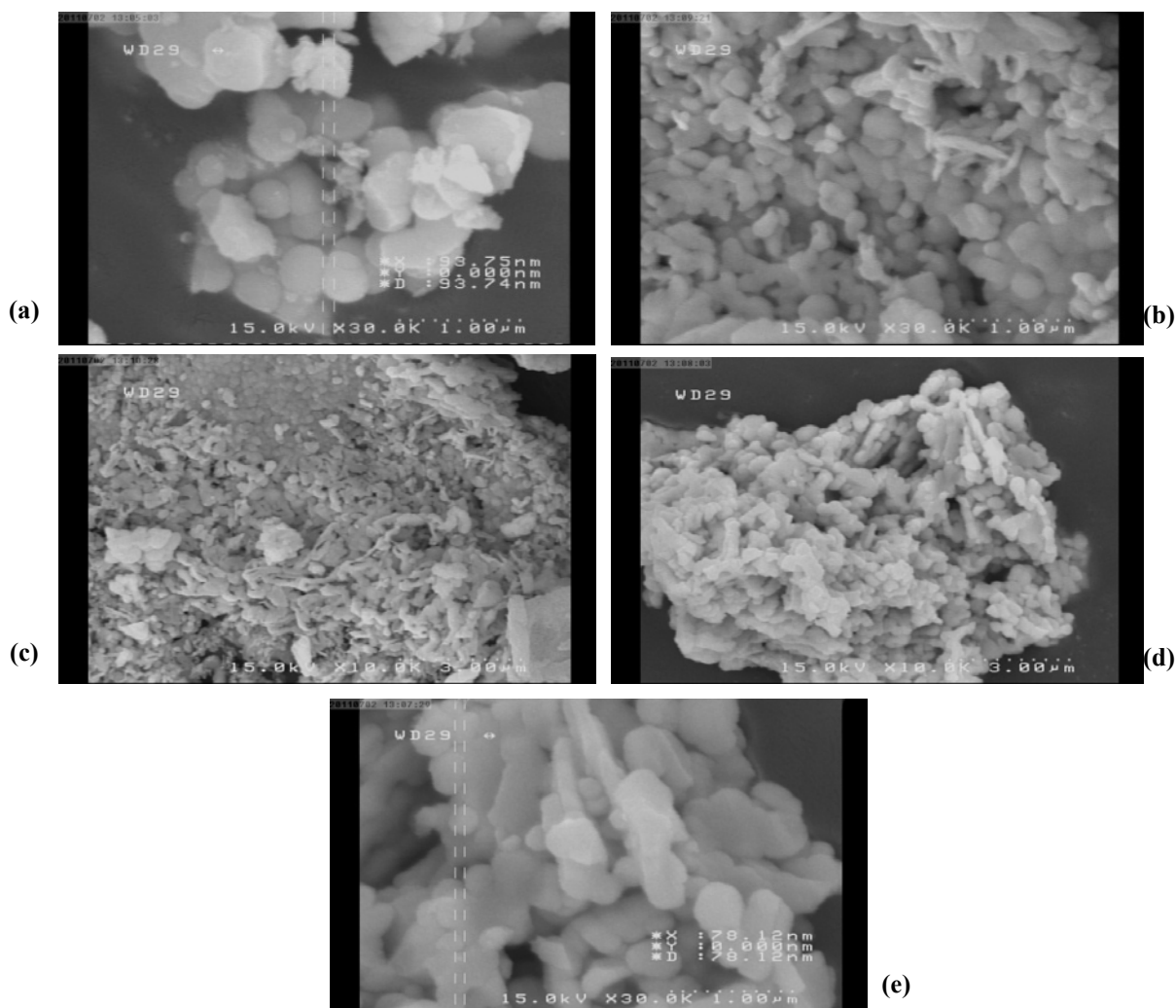
**Figure 4.** XRD patterns of fresh synthesized CuO/CeO<sub>2</sub> catalysts.

Figure 5 shows the SEM images of the fresh CuO/CeO<sub>2</sub> catalysts. It is apparent that fresh CuO/CeO<sub>2</sub> presents the spheroid structure in a uniform size distribution. It was also observed with CuO loading varying from 5 to

10% CuO have different particle size. The CuO/CeO<sub>2</sub> synthesized catalysts formed a special and very homogeneous arrangement by impregnation-ultrasound method.

**Table 2.** The crystal size of prepared catalysts from Scherrer's equation.

Catalyst	Max. Peak Angle (2θ)	Crystal Size (nm)
%5 CuO/CeO <sub>2</sub>	28.66	31.12
%15 CuO/CeO <sub>2</sub>	28.41	31.07



**Figure 5.** SEM photographs of fresh CuO/CeO<sub>2</sub> catalysts (a, b) %10 CuO scale bar 1.00 μm (c, d) %7 CuO scale bar 3.00 μm (e) %5 CuO scale bar 1.00 μm.

The activity and selectivity obtained with the CuO/CeO<sub>2</sub> catalysts for the selective oxidation of CO in the presence of excess hydrogen were presented in Fig. 6 and Fig. 7. Figure 6 shows the effect of Cu loading of the catalysts on CO conversion in CO oxidation in the absence of CO<sub>2</sub> and H<sub>2</sub>O (1% CO, 1% O<sub>2</sub>, 50 H<sub>2</sub> and balance N<sub>2</sub>). Figure 6 presents the CO conversion of four impregnation-ultrasound prepared catalysts, namely 5% Cu, 7% Cu, 10% Cu and 15% Cu. The 7%Cu, 10%Cu catalysts appeared to be the most active. Comparable results were previously reported in the literature by Avgouropoulos et al. [25] who observed that, among their three CuO/CeO<sub>2</sub> prepared catalysts by co-precipitation, the 14.3 % Cu catalyst was more active than the 7.3 or 20.9% Cu catalysts in CO oxidation. Using a 30000 h<sup>-1</sup> gas hourly space velocity (GHSV), 100% CO conversion can be achieved at 100°C. As can be seen, the reactor is located outside the furnace. The reaction temperature is lower than the previous works [16, 19]. Figure 7 presents the CO selectivity of one impregnation-ultrasound prepared sample, namely 10% CuO. Using a 30000 h<sup>-1</sup> GHSV, it attained 100% CO conversion with 86% selectivity at 100°C. This catalyst exhibits very high activity and selectivity for PROX of CO in H<sub>2</sub>. Regardless of the presence of 50 vol. % H<sub>2</sub> in the feed, no H<sub>2</sub> at all was oxidized at temperatures lower than 60-80°C, indicating that the catalyst was almost inactive for the oxidation of H<sub>2</sub> in the low temperature regime. Nevertheless, the selectivity decreased gradually with the increase of reaction temperature.

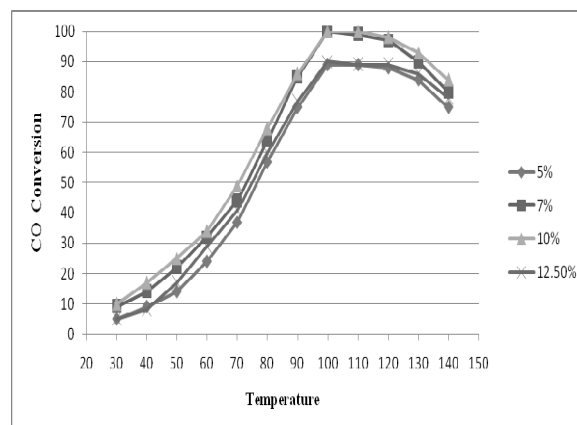


**Figure 6.** Variation of CO conversion with the reaction temperature for the selective oxidation of CO.

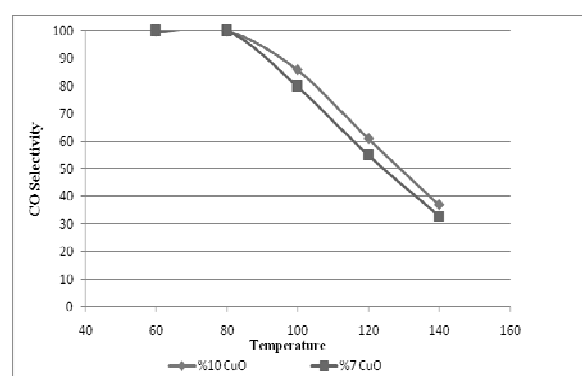


**Figure 7.** Variation of CO selectivity with the reaction temperature for the selective oxidation of CO.

#### 4. Conclusions

CuO/CeO<sub>2</sub> catalysts, with Cu loading in the range 5–15 wt% were prepared by impregnation-ultrasound method, and studied in both the CO oxidation and the selective CO oxidation in excess hydrogen. The following main conclusions may be drawn from this research:

The BET, XRD and SEM results indicate that CuO/CeO<sub>2</sub> particles are nano-structured catalysts. XRD invisible CuO species were synthesized with ultrasound method of the CuO phase on the ceria confirmed in high percentages. FTIR analysis exhibited functional group Cu-O bond in the catalysts.

SEM analysis indicated CuO/CeO<sub>2</sub> catalysts containing highly dispersed. The pilot was designed so that, reactor was out of the furnace. The impregnation-ultrasonic CuO/CeO<sub>2</sub> catalysts are very active and remarkably selective for the CO oxidation in the presence of excess hydrogen. CO conversion higher than 99% with selectivity of 86% can be obtained for this CuO/CeO<sub>2</sub> catalyst at 90–110 °C and a space velocity of 30,000h<sup>-1</sup> in the absence of CO<sub>2</sub> and H<sub>2</sub>O.

### Nomenclature

*D* the crystalline size

$\lambda$  the X-ray wavelength

$\beta$  the line broadening at half the maximum intensity (FWHM)

### References

- [1] Marschner, F. and Moeller, F.W., Methanol Synthesis, Applied Industrial Catalysis, Academic Press in: B.E. Leach (Ed.), 215, (1983).
- [2] Qi, Z., He, C. and Kaufman, A., "CO tolerance of low-loaded Pt/Ru anodes for PEM fuel cells", *J. Power Sources*, 111, 239, (2002).
- [3] Shore, L., Farrauto, R.J., Vielstich, W. and et al., Handbook of Fuel Cells-Fundamentals, Vol. 3, Wiley Publishers, 211, Chapter 18, (2003).
- [4] Tanaka, H., Kuriyama, M., Ishida, Y., Tomishige, K. and Kunimori, K., Part I. Catalytic performance, *Appl. Catal. A.*, 343, 117, (2008).
- [5] Shen, W.J., Ichihashi, Y., Ando, H., Matsumura, Y. and Haruta, M., "Effect of reduction temperature on structural properties and CO/CO<sub>2</sub> hydrogenation characteristics of a Pd-CeO<sub>2</sub> catalyst" , *Appl. Catal. A.*, 217, 231, (2001).
- [6] Pozdnyakova, O., Teschner, D., Wootsch, A. and et al., "Preferential CO oxidation in hydrogen (PROX) on ceria-supported catalysts, Part II: oxidation states and surface species on Pd/CeO<sub>2</sub> under reaction conditions, suggested reaction mechanism", *J. Catal.*, 237, 17, (2006).
- [7] Chin, S.Y., Alexeev, O.S. and Amiridis, M.D. "Preferential oxidation of CO under excess H<sub>2</sub> conditions over Ru catalysts", *Appl. Catal. A.*, 286, 157, (2005).
- [8] Han, Y.F., Kahlich, M.J., Kinne, M. and Behm, R.J., "CO removal from realistic methanol reformat via preferential oxidation – performance of a Rh/MgO catalyst and comparison to Ru/ $\gamma$ -Al<sub>2</sub>O<sub>3</sub> and Pt/ $\gamma$ -Al<sub>2</sub>O<sub>3</sub>", *Appl. Catal. B.*, 50, 209, (2004).
- [9] Chang, L.H., Sasirekha, N. and Chen, Y.W., "Au/MnO<sub>2</sub>-TiO<sub>2</sub> catalyst for preferential oxidation of carbon monoxide in hydrogen stream", *Catal. Commun.*, 8, 1702, (2007).
- [10] Deng, W.L., and Jesus, J.D., Saltsburg, H. and Flytzani-Stephanopoulos, M., "Low-content gold-ceria catalysts for the water gas shift and preferential CO oxidation reactions", *Appl. Catal. A.*, 291, 126, (2005).
- [11] Wang, H., Zhu, H.Q., Qin, Z.F., Wang, G.F., Liang, F.X. and Wang, J.G. "Preferential oxidation of CO in H<sub>2</sub> rich stream over Au/CeO<sub>2</sub>-Co<sub>3</sub>O<sub>4</sub>", *Catal. Commun.*, 9, 1487, (2008).
- [12] Teng, Y., Sakurai, H., Ueda, A. and Kobayashi, T., "Oxidative removal of CO contained in hydrogen by using metal oxide catalysts", *Int. J. Hydrogen Energy*, 24, 355, (1999).
- [13] Guo, Q. and Liu, Y., "MnOx modified Co<sub>3</sub>O<sub>4</sub>-CeO<sub>2</sub> catalysts for the preferential oxidation of CO in H<sub>2</sub>-rich gases", *Appl. Catal. B.*, 82, 19, (2008).



- [14] Kang, M., Song, M.W. and Lee, C.H., "Catalytic carbon monoxide oxidation over CoOx/CeO<sub>2</sub> composite catalysts", *Appl. Catal. A.*, 251, 143, (2003).
- [15] Cheekatamarla, P.K., Epling, W.S. and Lane, A.M., "Catalytic Autothermal Reforming of Diesel Fuel for Hydrogen Generation in Fuel Cells", *J. Power Sources*, 147, 178, (2005).
- [16] Avgouropoulos, G., Ioannides, T. and Matralis, H., "Influence of the preparation method on the performance of CuO-CeO<sub>2</sub> catalysts for the selective oxidation of CO", *Appl. Catal. B: Environ.*, 56, 87, (2005).
- [17] Marbáñ, G. and Fuertes, A.B., "A general and low-cost synthetic route to high-surface area metal oxides through a silica xerogel template", *Appl. Catal. B: Environ.*, 57, 43, (2005).
- [18] Kanani Harandi, M., Alizadeh, R. and Fatehifar, E., "Synthesis and characterization of sulfur dioxide hydrogenation nanocatalysts", M.Sc. thesis, 58, (2010).
- [19] Sedmak, G., Hočevcar, S. and Levec, J., "Kinetics of selective CO oxidation in excess of H<sub>2</sub> over the nanostructured Cu<sub>0.1</sub>Ce<sub>0.9</sub>O<sub>2-y</sub> catalyst", *Journal of Catalysis*, 213, 135, (2003).
- [20] Pouretdal, H.R. and Kadkhodaie, A., "Synthetic CeO<sub>2</sub> nanoparticle catalysis of methylene blue photodegradation: Kinetics and mechanism", *Chin. J. Catal.*, 31, 1328, (2010).
- [21] Zhang, J. and Ostrovski, O., "Iron ore reduction/ cementation experimental results and kinetic modeling", *Iron-making and Steelmaking*, 29, (2002).
- [22] Liu, W. and Flytzani-Stephanopoulos, M., "Transition metal/fluorite-type oxides as active catalysts for reduction of sulfur dioxide to elemental sulfur by carbon monoxide *Chemical Engineering*", *J. Catal.*, 153, 304, (1995).
- [23] Zheng, X., Wang, Sh., Zhang, S. Wang, S., Huang, W. and Wu, S., "Characterization and CO oxidation Catalytic behaviour of CuO/CeO", *Reaction Kinetics and Catalysis Letters*, 84, 29, (2005).
- [24] Zhang, S., Huang, W., Qiu, X., Li, B., Zheng, X. and Wu, S., "Comparative study on catalytic properties for Low-temperature CO oxidation of Cu/CeO<sub>2</sub> and CuO/CeO<sub>2</sub> prepared via solvated metal atom impregnation and conventional impregnation", *Catal. Lett.*, 80, 41, (2002).
- [25] Avoguropoulos, G., Ioannides, T., Matralis, H.K., Batista, J. and Hočevcar, S., "CuO/CeO<sub>2</sub> mixed oxide catalysts for the selective oxidation of carbon monoxide in excess hydrogen", *Catal. Lett.*, 73, 33, (2001).